Dalton Transactions

Dynamic Article Links

Cite this: *Dalton Trans.*, 2011, **40**, 8059

www.rsc.org/dalton

PERSPECTIVE

Enthalpy–entropy correlations as chemical guides to unravel self-assembly processes

Claude Piguet*

Received 12th January 2011, Accepted 12th April 2011
DOI: 10.1039/c1dt10055f

Intermolecular connections play a crucial role in biology (recognition, signalling, binding), in physics (material cohesion) and in chemistry ((supra)molecular engineering). While a phenomenological thermodynamic free-energy approach for modelling self-assemblies is now at hand, a more satisfying description based on the chemically-intuitive enthalpic and entropic contributions remains elusive. On the other hand, the innumerable reports of empirical enthalpy/entropy correlations characterizing intermolecular interactions justify a questioning about the emergence and exploitation of an apparent 'fourth law of thermodynamics', which could provide a simple manipulation of intermolecular binding processes. This tutorial Perspective aims at highlighting the current level of non-quantum rationalization of enthalpy–entropy correlations and their chemical consequences on the tuning and on the programming of intermolecular interactions in pure materials, and in diluted solutions.

1. The thermodynamic free-energy model for simple intermolecular associations

The modelling of the sequential intermolecular binding of i ligands B onto a receptor A represents one of the first challenge addressed by classical thermodynamics at the turn of the 19th century. The associated cumulative stability constant $\beta_{1,i}^{A,B}$ can be expressed in eqn (1) within the frame of the van't Hoff isotherm using a standard concentration c^{θ} for the reference state of each partner ($|A|$, $|B|$ and $|[AB_i]|$ are the molar concentrations of the incriminated species).[1]

$$A + iB \rightleftharpoons [AB_i]$$

$$\Delta G_{1,i}^{A,B} = -RT \ln\left(\beta_{1,i}^{A,B}\right) = -RT \ln\left(\frac{|[AB_i]|}{|A||B|^i}\left(c^{\theta}\right)^i\right) \quad (1)$$

Assuming that the receptor A has n available and identical binding sites, $\beta_{1,i}^{A,B}$ can be theoretically modelled by the combination of a binomial coefficient $C_i^n = n!/(n-i)!i!$, which represents the purely entropic statistical factor of the assembly (*i.e.* the number of possible arrangements of i ligands B among the n equivalent sites) with the thermodynamic microscopic affinity $k^{A,B}$ for a single intermolecular A–B connection ($\Delta G_{inter}^{A,B} = -RT \ln(k^{A,B})$, eqn (2)).[2]

$$\beta_{1,i}^{A,B} = C_i^n (k^{A,B})^i \quad (2)$$

Obviously, A and B hold for any receptor/substratum pair which could be found in biology (protein/ligand, effector/receptor, *etc.*), in physics (cation/anion in ionic solids, micro-cohesion in material, *etc.*) or in chemistry (metal/ligand, host/guest, *etc.*). The consideration of the occupancy factor μ (eqn (3), left), followed by the introduction of the pertinent mass balances provides mathematical sums which can be easily transformed into polynomials (eqn (3), centre). Straightforward simplifications eventually yields the classical Langmuir binding isotherm (eqn (3), right).[2] For the sake of clarity, the well-accepted standard concentration of c^{θ} = 1 M is systematically used for the reference state along this tutorial Perspective.[3]

Department of Inorganic, Analytical and Applied Chemistry, University of Geneva, 30 quai Ernest Ansermet, CH-1211, Geneva 4. E-mail: Claude.Piguet@unige.ch; Fax: (41 22) 379 6830; Tel: (41 22) 379 6034

Claude Piguet

Claude Piguet earned a PhD degree in 1989 in the field of biomimetic copper–dioxygen complexes. After postdoctoral periods in the groups of professors J.-M. Lehn, A. F. Williams and J.-C. G. Bünzli, he initiated research projects in the field of lanthanide supramolecular chemistry. He received the Werner Medal of the New Swiss Chemical Society (1995) and was appointed in as a full professor of inorganic chemistry at the University of Geneva (1999). He has co-authored more than 150 scientific articles addressing various aspects of basic chemistry and physics. In 2009, he was awarded the Lecoq de Boisbaudran Senior Award from the European Rare Earth Society.

$$\mu = \frac{|\mathrm{B}|_{\mathrm{bound}}}{|\mathrm{A}|_{\mathrm{tot}}} = \frac{|\mathrm{B}|_{\mathrm{tot}} - |\mathrm{B}|}{|\mathrm{A}|_{\mathrm{tot}}} = \frac{\sum_{i=1}^{n} i\left[\mathrm{AB}_i\right]}{|\mathrm{A}| + \sum_{i=1}^{n}\left[\mathrm{AB}_i\right]} =$$
$$\frac{\sum_{i=1}^{n} i\beta_i^{\mathrm{A,B}}|\mathrm{B}|^i}{1+\sum_{i=1}^{n}\beta_i^{\mathrm{A,B}}|\mathrm{B}|^i} = \frac{\sum_{i=1}^{n} iC_i^n\left(k^{\mathrm{A,B}}\right)^i|\mathrm{B}|^i}{1+\sum_{i=1}^{n}C_i^n\left(k^{\mathrm{A,B}}\right)^i|\mathrm{B}|^i} = \frac{nk^{\mathrm{A,B}}|\mathrm{B}|}{1+k^{\mathrm{A,B}}|\mathrm{B}|} \quad (3)$$

Two famous linear forms of eqn (3), known as the Hill plot ($\ln(\mu/(n-\mu))$ *vs.* $\ln(|\mathrm{B}|)$, eqn (4)),[4] and the Scatchard plot ($\mu/|\mathrm{B}|$ *vs.* μ, eqn (5)),[5] have been extensively used for estimating $k^{\mathrm{A,B}}$ during a titration procedure, in which $|\mathrm{B}|$ can be experimentally measured for various compositions of the mixture ($|\mathrm{A}|_{\mathrm{tot}}/|\mathrm{B}|_{\mathrm{tot}}$). When $k^{\mathrm{A,B}}$ does not change with the number of ligands B coordinated to A, plots according to eqn (4) and (5) display straight lines and the process is said to be non-cooperative or statistical.

$$\ln(\mu/(n-\mu)) = \ln(|\mathrm{B}|) + \ln(k^{\mathrm{A,B}}) \quad (4)$$

$$\mu/|\mathrm{B}| = -k^{\mathrm{A,B}}\mu + nk^{\mathrm{A,B}} \quad (5)$$

Any deviation of these plots from linearity can be assigned to some changes of $k^{\mathrm{A,B}}$ with the number of ligands i, a phenomenon termed cooperativity (positive cooperativity is characterized by an increase of $k^{\mathrm{A,B}}$ with i, while negative cooperativity holds for the reverse situation).[6] The origin of non-statistical behaviour (*i.e.* cooperativity) is usually assigned to the operation of a non-zero intramolecular homo-component free-energy term $\Delta E^{\mathrm{B,B}}$, sometimes referred to as the allosteric factors.[7] Any stability micro-constant $\beta_{\{si\}}^{\mathrm{A,B}}$ characterizing the formation of a purely intermolecular $[\mathrm{AB}_i]$ assembly (eqn (1)) can be thus modelled with eqn (6), where each state vector $\{s_i\}$ contains n elements with $s_m = 1$ when the mth binding site of the receptor A in the $[\mathrm{AB}_i]$ microspecies is occupied by a ligand B, and $s_m = 0$ occurs when no ligand is bound. The homo-component B–B interaction operating between sites m and p is taking into account by the Boltzmann factor $u_{m,p}^{\mathrm{B,B}} = \mathrm{e}^{-\Delta E_{m,p}^{\mathrm{B,B}}/RT}$ (eqn (6)), and the global macro-constant is obtained by a trivial sum over all micro-constants (eqn (7)).[7]

$$\beta_{\{s_i\}}^{\mathrm{A,B}} = \prod_{m=1}^{n}\left(k_m^{\mathrm{A,B}}\right)^{s_m}\prod_{m<p}^{n}\mathrm{e}^{-\left(\Delta E_{m,p}^{\mathrm{B,B}}/RT\right)^{s_m s_p}} = \prod_{m=1}^{n}\left(k_m^{\mathrm{A,B}}\right)^{s_m}\prod_{m<p}^{n}\left(u_{m,p}^{\mathrm{B,B}}\right)^{s_m s_p} \quad (6)$$

$$\beta_i^{\mathrm{A,B}} = \sum_{\{s_i\}}\beta_{\{s_i\}}^{\mathrm{A,B}} \quad (7)$$

Although eqn (6) and (7) may frighten the broad chemical audience concerned by a Perspective in Dalton Transactions, they indeed rigorously describe the very simple energetic change brought by the successive intermolecular chemical binding of i ligands B to a single receptor A possessing a maximum of n binding sites, according that the fixation of each B ligand may affect the entry of the next one by a free-energy correction term $\Delta E^{\mathrm{B,B}}$. As often in chemistry, the application of apparently complicated equations to simple examples greatly facilitates their acceptance. Let's then illustrate this approach for the replacement of two water molecules with two ammonia ligands around divalent octahedral Ni(II) in equilibrium (8).

$$[\mathrm{Ni(H_2O)_6}]^{2+} + 2\mathrm{NH_3} \rightleftharpoons [\mathrm{Ni(H_2O)_4(NH_3)_2}]^{2+} + 2\mathrm{H_2O}:\ \beta_{1,2}^{\mathrm{Ni,NH3}} \quad (8)$$

Since there are two microspecies (*cis*-$[\mathrm{Ni(H_2O)_4(NH_3)_2}]^{2+}$, statistical factor $\omega_{1,2,cis}^{\mathrm{Ni,NH3}} = 12$; and *trans*-$[\mathrm{Ni(H_2O)_4(NH_3)_2}]^{2+}$, statistical factor $\omega_{1,2,trans}^{\mathrm{Ni,NH3}} = 3$)[8] contributing to the macrospecies $[\mathrm{Ni(H_2O)_4(NH_3)_2}]^{2+}$, the modelling of each micro-constant with eqn (6) gives

$$\beta_{1,2,cis}^{\mathrm{Ni,NH3}} = 12(k^{\mathrm{Ni,NH3}})^2 u_{cis}^{\mathrm{Ni,NH3}} \quad (9)$$

$$\beta_{1,2,trans}^{\mathrm{Ni,NH3}} = 3(k^{\mathrm{Ni,NH3}})^2 u_{trans}^{\mathrm{Ni,NH3}} \quad (10)$$

Their combination into a single macro-constant according to eqn (7) eventually yields

$$\beta_{1,2}^{\mathrm{Ni,NH3}} = 12(k^{\mathrm{Ni,NH3}})^2 u_{cis}^{\mathrm{Ni,NH3}} + 3(k^{\mathrm{Ni,NH3}})^2 u_{trans}^{\mathrm{Ni,NH3}} = (k^{\mathrm{Ni,NH3}})^2(12u_{cis}^{\mathrm{Ni,NH3}} + 3u_{trans}^{\mathrm{Ni,NH3}}) \quad (11)$$

If one considers that (i) the macro-constants for the successive fixations of up to six ammonia molecules to Ni(II) are experimentally accessible ($\beta_{1,i}^{\mathrm{Ni,NH3}}$, $i = 1$–6), and that (ii) each macro-constant is easily modelled by using eqn (6) and (7) with the exclusive use of the same three parameters $k^{\mathrm{Ni,NH3}}$, $u_{cis}^{\mathrm{Ni,NH3}}$ and $u_{trans}^{\mathrm{Ni,NH3}}$, a straightforward non-linear least-square fit (six equations, three parameters) provides the best free-energy parameters $\Delta G_{\mathrm{inter}}^{\mathrm{Ni,NH3}} = -RT\ln(k^{\mathrm{Ni,NH3}}) = -11.70(6)$ kJ mol^{-1}, $\Delta E_{cis}^{\mathrm{Ni,NH3}} = -RT\ln(u_{cis}^{\mathrm{Ni,NH3}}) = 1.35(2)$ kJ mol^{-1} and $\Delta E_{trans}^{\mathrm{Ni,NH3}} = -RT\ln(u_{trans}^{\mathrm{Ni,NH3}}) = 1.33(2)$ kJ mol^{-1}.[9] The positive values found for the allosteric factors $\Delta E_{cis}^{\mathrm{Ni,NH3}}$ and $\Delta E_{trans}^{\mathrm{Ni,NH3}}$ indicate that the sequential replacement of water molecules with ammonia around Ni(II) follows an anti-cooperative protocol. However, its origin in term of electronic or steric effects remains elusive in absence of a reliable dissection of these free energy terms into chemically accessible enthalpic and entropic contributions.[10] The latter limitation is even more dramatic for the interpretation of the microscopic free energy $\Delta G_{\mathrm{inter}}^{\mathrm{Ni,NH3}}$ characterizing each Ni–$\mathrm{NH_3}$ connection, since any intermolecular assembly in solution indeed corresponds to a two-step mechanism where the initial desolvation step is followed by a pure association process (Fig. 1).[11] We can thus write

$$\Delta G_{\mathrm{inter}}^{\mathrm{A,B}} = -RT\ln(k^{\mathrm{A,B}}) = \Delta G_{\mathrm{desolv}}^{\mathrm{A,B,S}} + \Delta G_{\mathrm{asso}}^{\mathrm{A,B}} \quad (12)$$

We now easily realize that the free energy change accompanying any assembly process performed in solution is indeed a balance between successive dissociation (*i.e.* desolvation) and association steps. This difficulty is further amplified when the enthalpic and entropic contributions are derived with the help of the Gibbs–Helmholtz relationship (eqn (13)–(15) in Fig. 1). The free-energy change in each step is itself a balance between two opposite contributions ($\Delta H_{\mathrm{desolv}}^{\mathrm{A,B,S}} > 0$ while $-T\Delta S_{\mathrm{desolv}}^{\mathrm{A,B,S}} < 0$ in eqn (13) and $\Delta H_{\mathrm{asso}}^{\mathrm{A,B}} < 0$ while $-T\Delta S_{\mathrm{asso}}^{\mathrm{A,B}} > 0$ in eqn (14)), while the global enthalpic $\Delta H_{\mathrm{inter}}^{\mathrm{A,B}} = \Delta H_{\mathrm{desolv}}^{\mathrm{A,B,S}} + \Delta H_{\mathrm{asso}}^{\mathrm{A,B}}$ and entropic $\Delta S_{\mathrm{inter}}^{\mathrm{A,B}} = \Delta S_{\mathrm{desolv}}^{\mathrm{A,B,S}} + \Delta S_{\mathrm{asso}}^{\mathrm{A,B}}$ contributions (eqn (15)) again result from the combinations of terms with opposite signs.[10] In order to establish some chemical correlations between the thermodynamics of intermolecular

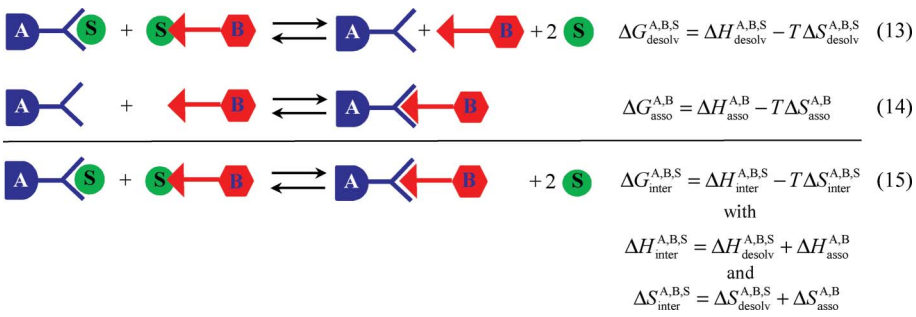

Fig. 1 Choppin's model for the two-step mechanism responsible for standard intermolecular hetero-component connections in solution (S is a solvent molecule).[10]

interactions and the stereo-electronic structures of the molecular partners, the explicit dissection of each process into enthalpic and entropic contributions is thus crucial. Encouraged by the heading of this invited contribution as a 'Perspective', we propose a critical but chemically-intuitive approach to the concept of enthalpy/entropy correlation,[12] which can be considered as a guide for a deeper interpretation of self-assembly processes occurring in pure materials (in absence of solvent) or in diluted solution (in presence of solvent).

2. Modelling the enthalpic and entropic contributions in intermolecular associations

There is a common belief in chemistry that the change in dynamics accompanying a simple intermolecular association (measured by $\Delta S^{A,B}_{asso} < 0$ in eqn (14) is correlated with the strength in bonding (measured by $\Delta H^{A,B}_{asso} < 0$ in eqn (14)).[13] The innumerable experimental reports of such enthalpy/entropy compensations observed in biology, physics and chemistry strongly support this axiomatic statement.[12–14] Moreover, the classical chelate enhancement of binding of Jencks[15] similarly claims that the entropic cost ($T\Delta S_{asso}$) for the association of A and B is some fraction of 50–60 kJ mol^{-1}, and it is a sensitive function of the exothermicity of the interaction.[16] Though there is no 'fourth law of thermodynamics' which could theoretically justify enthalpy/entropy compensation (later written H/S compensation in the following), there were some noticeable efforts for rationalizing weak intermolecular interactions with the help of simple Lennard-Jones potentials, in which the depth of the electrostatic well, responsible for the intermolecular association would be correlated with the density of states (Fig. 2).[13] Simply speaking, the basic idea links a deep electrostatic well ($\Delta H^{A,B}_{asso} \ll 0$) with relatively little motion ($\Delta S^{A,B}_{asso} \ll 0$) because the density of states is too small for being populated at room temperature (Fig. 2a). The reverse situation holds for a looser association between the A and B partners (Fig. 2b).[13b] A supporting theoretical model was proposed by Dünitz in 1995, which indeed strictly predicted positive H/S correlations (*i.e.* compensation effects).[17] However, the simulated enthalpy–entropy curve was generated by the variation of the energy parameter (*i.e.* the well depth) while the size parameter (*i.e.* the most probable bond length) was held fixed. This limitation is probably responsible for discarding negative H/S correlation (*i.e.* anti-compensation, see next section), a phenomenon also encountered in the literature, and unambiguously established in chemistry.[18]

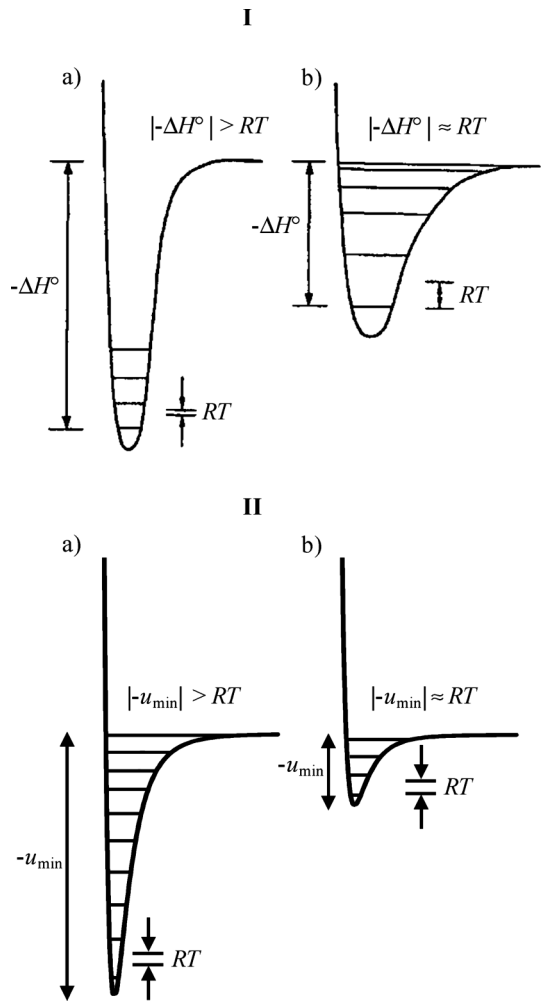

Fig. 2 (I) Original schematic illustration for an electrostatic potential well in which (a) the enthalpy of dissociation of a complex is large compared with RT (thermal energy at room temperature) and (b) the enthalpic barrier to dissociation is comparable to, or several times, RT.[13b] Reproduced by permission of The Royal Society of Chemistry. (II) Quantitative drawing of the same phenomenon with the help of Lennard-Jones (12,6) potentials and anharmonic vibrational levels combined with eqn (24), which is responsible for the emergence of H/S compensation (r_0 is constant).

In order to get rid of debatable assumptions, Ford[18] followed the formalism of molecular association proposed by Luo and Sharp,[19] that is traced back to Bjerrum's model. If the receptor A is assumed

to be fixed near the origin, the equilibrium constant $K_{asso}^{A,B}$ for the association process described in eqn (14) is given by eqn (16), whereby r and Ω are the position, respectively the orientation of B, $\beta = (k_b T)^{-1}$ is the thermal factor with k_b being the Boltzmann's constant and T being the temperature, ω is the potential mean force between A and B, and $H(r, \Omega)$ is a bonding function that is $H(r, \Omega) = 1$ when complex [AB] exists and $H(r, \Omega) = 0$ otherwise (Fig. 3).[18,19]

$$K_{asso}^{A,B} = \frac{|[AB]|}{|A||B|} = \frac{c^{\theta}}{8\pi^2}\int H(r,\Omega)\cdot e^{-\beta\omega(r,\Omega)}dr\ d\Omega \qquad (16)$$

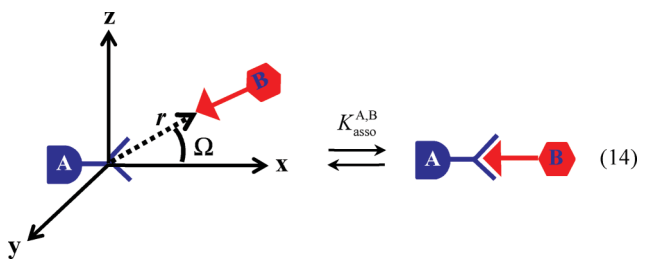

(14)

Fig. 3 Schematic illustration of Bjerrum's model for the intermolecular process depicted in eqn (14).

Neglecting any specific internal structure for A and B, the potential mean force simplifies to $\omega(r, \Omega) = u(r)$ and only depends on the scalar distance r between the centres of mass. Moreover, we will assume that $u(r) = u_{min}^{A,B} + (\kappa^{A,B}/2)r^2$ is a straightforward harmonic potential with the energy minimum $u_{min}^{A,B}$ located at $r = 0$ (Fig. 3) and with a force constant $\kappa^{A,B}$. Following Luo and Sharp, $H(r, \Omega) = 1$ over all space since the Boltzmann's factor $e^{-\beta\left(u_{min}^{A,B}+\left(\kappa^{A,B}/2\right)r^2\right)}$ in eqn (16) will vanish for high energy configurations anyway (*i.e.* unbound states with large r distance). With these assumptions, Ford showed that the integral in eqn (16) gave[18]

$$K_{asso}^{A,B} = c^{\theta}\left(\frac{2\pi}{\beta\kappa^{A,B}}\right)^{3/2} e^{-\beta u_{min}^{A,B}} \qquad (17)$$

The use of the van't Hoff isotherm transforms the association constant into its associated free energy.[3]

$$\begin{aligned}\Delta G_{asso}^{A,B} &= -k_b T \ln\left(K_{asso}^{A,B}\right) = -\frac{1}{\beta}\ln\left[c^{\theta}\left(\frac{2\pi}{\beta\kappa^{A,B}}\right)^{3/2} e^{-\beta u_{min}^{A,B}}\right] \\ &= u_{min}^{A,B} - k_b T \ln\left[c^{\theta}\left(\frac{2\pi}{\beta\kappa^{A,B}}\right)^{3/2}\right]\end{aligned} \qquad (18)$$

Taking into account the change in the number of translational degrees of freedom accompanying the association process, the application of the Gibbs–Helmholtz relationship to eqn (18) yields[18]

$$\Delta H_{asso}^{A,B} = u_{min}^{A,B} + \frac{3}{2}k_b T \qquad (19)$$

$$\Delta S_{asso}^{A,B} = k_b \ln\left[c^{\theta}\left(\frac{2\pi e}{\beta\kappa^{A,B}}\right)^{3/2}\right] \qquad (20)$$

In complete agreement with chemical intuition for an intermolecular connection controlled by a single harmonic potential,[13,20] the enthalpic contribution $\Delta H_{asso}^{A,B}$ only depends on the well depth of the interaction ($u_{min}^{A,B}$ in eqn (19)). Obviously, the entropic contribution $\Delta S_{asso}^{A,B}$ depends on the original choice of the standard state (c^{θ} in eqn (20)),[3] but its magnitude is further modulated by the force constant of the interaction ($\kappa^{A,B}$ in eqn (20)). To the best of our knowledge, there is however no fundamental principle of weak interactions that dictates the relative dependence of well depth $u_{min}^{A,B}$ and force constant $\kappa^{A,B}$, hence justifying a special thermodynamic relationship between $\Delta H_{asso}^{A,B}$ and $\Delta S_{asso}^{A,B}$. One can however deduce from eqn (19) and (20) that, if a perturbation is applied to the molecular [AB] pairs such that $u_{min}^{A,B}$ and $\kappa^{A,B}$ move in the opposite direction, the result will be H/S compensation, *i.e.* $\Delta H_{asso}^{A,B}$ and $\Delta S_{asso}^{A,B}$ both decrease, or both increase. When $u_{min}^{A,B}$ and $\kappa^{A,B}$ move in the same direction, anti-compensation occurs.

3. Enthalpy–entropy compensation in intermolecular associations: a 'hidden' structural constraint

Following the simple (non-quantum) model catching the physical forces responsible for the formation of a molecular [AB] pair, an intermolecular interaction (equilibrium (14) can be modeled with a simple Lennard-Jones (12,6) potential V_{LJ}, which resorts to only two parameters: (i) the absolute minimum of the attractive well depth ε and (ii) the minimum intermolecular A···B distance r_0 at which the potential of the interaction is zero (eqn (21) and Fig. 4).[20]

$$V_{LJ}(r) = 4\varepsilon\left[\left(r_0/r\right)^{12} - \left(r_0/r\right)^{6}\right] \qquad (21)$$

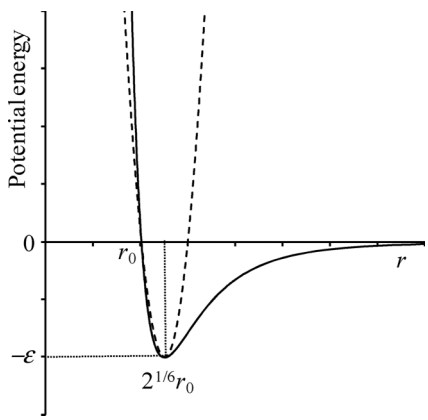

Fig. 4 Representation of a Lennard-Jones (12,6) potential (full trace) with the interpretation of ε and r_0 parameters, and its harmonic approximation (eqn (22), dashed trace) modeling the intermolecular interactions operating in a [AB] complex.

While the correlation between the well depth and the harmonic potential used for obtaining eqn (18) is trivial and $\varepsilon = -u_{min}^{A,B}$, an analytical formulation of the force constant $\kappa^{A,B}$ as a function of ε and r_0 requires the development of the harmonic potential V_{harm} at the minimum of the Lennard-Jones attractive well.[18] The application of the three conditions V_{harm} ($r = r_0$) = 0, dV_{harm} ($r = 2^{1/6}r_0$)/$dr = 0$ and $V_{harm}(r = 2^{1/6}r_0) = -\varepsilon$ leads to (Fig. 4).[21]

$$V_{\mathrm{harm}}(r) = \frac{\varepsilon}{\lambda}\left[-2^{-7/6}\left(r/r_0\right)^2 + \left(r/r_0\right) + 2^{-7/6} - 1\right] \text{ with} \quad (22)$$
$$\lambda = 2^{-7/6} - 2^{-1/6} - 2^{-7/6} + 1$$

Since the total energy of the harmonic oscillator for the motion amplitude $A = r_0(1-2^{1/6})$ amounts to ε (Fig. 4), we can simply write

$$\varepsilon = \frac{\kappa^{\mathrm{A,B}}\left[r_0\left(1-2^{1/6}\right)\right]^2}{2} \Rightarrow \kappa^{\mathrm{A,B}} = \frac{2}{\left(1-2^{1/6}\right)^2}\cdot\frac{\varepsilon}{\left(r_0\right)^2} \quad (23)$$

which is eventually transformed into eqn (24) if we remind that $\varepsilon = -u_{\mathrm{min}}^{\mathrm{A,B}}$.

$$\kappa^{\mathrm{A,B}} = -\frac{2}{\left(1-2^{1/6}\right)^2}\cdot\frac{u_{\mathrm{min}}^{\mathrm{A,B}}}{\left(r_0\right)^2} \quad (24)$$

When the structural parameter r_0 is constant along a perturbation applied to the molecular [AB] pair (*i.e.* the minimum contact distance at which the interaction potential is zero is retained along the perturbation), eqn (24) predicts that the force constant $\kappa^{\mathrm{A,B}}$ controlling the association entropy (eqn (20)), and the well depth $u_{\mathrm{min}}^{\mathrm{A,B}}$ controlling the association enthalpy (eqn (19)) are indeed correlated.[18,21] This result, which implies a 'hidden' physicochemical process at the origin of H/S correlation[22] was recently theoretically justified for isobaric–isothermal partition functions with the help of statistical thermodynamics.[23] Assuming a minor perturbation of the system for which r_0 is fixed, eqn (24) becomes

$$\kappa^{\mathrm{A,B}} = -f\cdot u_{\mathrm{min}}^{\mathrm{A,B}} \text{ with } f = \left(2^{1/2}/\left(1-2^{1/6}\right)r_0\right)^2 > 0 \quad (25)$$

Consequently, any change of $u_{\mathrm{min}}^{\mathrm{A,B}}$ induces a shift of $\kappa^{\mathrm{A,B}}$ in the opposite direction and, reciprocally, any change of $\kappa^{\mathrm{A,B}}$ induces an opposite shift of $u_{\mathrm{min}}^{\mathrm{A,B}}$, which explains the frequent occurrence of H/S compensation when molecular systems are submitted to minor electronic and/or structural perturbations compatible with a constant value of r_0. The introduction of eqn (25) into eqn (19) yields

$$\Delta H_{\mathrm{asso}}^{\mathrm{A,B}} = -\frac{\kappa^{\mathrm{A,B}}}{f} + \frac{3}{2}k_{\mathrm{b}}T \Rightarrow \kappa^{\mathrm{A,B}} = f\left(\frac{3}{2}k_{\mathrm{b}}T - \Delta H_{\mathrm{asso}}^{\mathrm{A,B}}\right) \quad (26)$$

Moreover, such minute perturbations only moderately affect the average global force constant of the interaction around its average magnitude $\kappa_0^{\mathrm{A,B}}$. The use of the linear development $\ln\left(\kappa^{\mathrm{A,B}}\right) \simeq \ln\left(\kappa_0^{\mathrm{A,B}}\right) + \left(\left(\kappa^{\mathrm{A,B}} - \kappa_0^{\mathrm{A,B}}\right)/\kappa_0^{\mathrm{A,B}}\right)$ is thus justified in eqn (20) (first-order Taylor series), and eqn (27) can be easily obtained.

$$\Delta S_{\mathrm{asso}}^{\mathrm{A,B}} = k_{\mathrm{b}}\ln\left[c^{\theta}\left(\frac{2\pi e}{\beta\kappa_0^{\mathrm{A,B}}}\right)^{3/2}\right] + \frac{3}{2}k_{\mathrm{b}}\left(1-\frac{\kappa^{\mathrm{A,B}}}{\kappa_0^{\mathrm{A,B}}}\right) \quad (27)$$

The ultimate combination of eqn (26) into (27) followed by some simple, but tedious algebraic transformations, provides the linear correlation shown in eqn (28)–(30), sometimes referred to as 'strict H/S correlations' or as 'strong forms of H/S correlation'.[24]

$$\Delta H_{\mathrm{asso}}^{\mathrm{A,B}} = a\Delta S_{\mathrm{asso}}^{\mathrm{A,B}} + b \quad (28)$$

with

$$a = \frac{2\kappa_0^{\mathrm{A,B}}}{3k_{\mathrm{b}}f} = \frac{\left(1-2^{1/6}\right)^2\left(r_0\right)^2\kappa_0^{\mathrm{A,B}}}{3k_{\mathrm{b}}} \quad (29)$$

and

$$b = \frac{9k_{\mathrm{b}}Tf - 4\kappa_0^{\mathrm{A,B}}\left\{\ln\left[c^{\theta}\left(\frac{2k_{\mathrm{b}}T\pi e}{\kappa_0^{\mathrm{A,B}}}\right)^{3/2}\right] + \frac{3}{2}\right\}}{6f} \quad (30)$$

We immediately notice that $a > 0$ and linear H/S compensation 'naturally' results for a series of association (or dissociation) processes for which (i) the structural arrangement (measured by r_0) is invariant and (ii) the force constant (measured by $\kappa_0^{\mathrm{A,B}}$) are not drastically affected and can be estimated by a linear expansion around its central value $\kappa_0^{\mathrm{A,B}}$. While the first condition affecting r_0 is crucial for rationalizing H/S correlations (see the following sections), the second limitation can be relaxed by increasing the global order of the Taylor series, as experimentally evidenced for the parabolic distortions of series of intermolecular connection processes spanning large domains of association enthalpies.[13]

4. Enthalpy–entropy compensation in the melting of pure solids

Single-step H/S compensations have been mainly investigated in melting processes involving solid → liquid or solid → liquid crystalline phase transitions (ΔG_{m}, ΔH_{m}, ΔS_{m}),[12,13,25] or during the reverse physical transformations where liquids or liquid crystals condensate to give some organized solid-state materials (ΔG_{asso}, ΔH_{asso}, ΔS_{asso}).[17,26] These processes can be roughly modelled by a simple homotropic *n*-merization reaction (eqn (31)) for which $\Delta G_{\mathrm{m}} = -\Delta G_{\mathrm{asso}}$, $\Delta H_{\mathrm{m}} = -\Delta H_{\mathrm{asso}}$ and $\Delta S_{\mathrm{m}} = -\Delta S_{\mathrm{asso}}$.

$$n\mathrm{A} \underset{\Delta G_{\mathrm{m}}}{\overset{\Delta G_{\mathrm{asso}}}{\rightleftharpoons}} \mathrm{A}_n \quad (31)$$

The justification for the abundant thermodynamic data reported for melting processes arises from the fact that the melting enthalpy, ΔH_{m}, together with the temperature dependence of the heat capacity C_{p} in solids, liquid crystals and liquids, can be experimentally obtained with high precision by using standard calorimetric techniques. The associated entropy change is deduced from the melting temperature by using $\Delta S_{\mathrm{m}} = \Delta H_{\mathrm{m}}/T_{\mathrm{m}}$.[27] The subsequent corrections for changes of ΔH_{m} and ΔS_{m} with temperature (seldom considered in the literature) eventually give the standard melting enthalpy ΔH_{m}^0 and entropy ΔS_{m}^0.[27] The most famous example concerns the melting of linear saturated hydrocarbons $\mathrm{C}_n\mathrm{H}_{2n+2}$ of increasing length ($n > 1$), in which two terminal methyl tripods are separated by an increasing number ($n-2$) of methylene rotors.[28] The plot of $\Delta H_{\mathrm{m}}^0(\mathrm{C}_n\mathrm{H}_{2n+2})$ *vs.* $\Delta S_{\mathrm{m}}^0(\mathrm{C}_n\mathrm{H}_{2n+2})$ indeed displays strict H/S compensation (Fig. 5a, eqn (32)).

$$\Delta H_{\mathrm{m}}^0(\mathrm{C}_n\mathrm{H}_{2n+2}) = 295(19)\Delta S_{\mathrm{m}}^0(\mathrm{C}_n\mathrm{H}_{2n+2}) - 7327(1400)\ \mathrm{J\ mol^{-1}} \quad (32)$$

The replacement of $\Delta H_{\mathrm{m}}^0(\mathrm{C}_n\mathrm{H}_{2n+2})$ and $\Delta S_{\mathrm{m}}^0(\mathrm{C}_n\mathrm{H}_{2n+2})$ with their opposite associative counterparts $\Delta H^0{}_{\mathrm{asso}}(\mathrm{C}_n\mathrm{H}_{2n+2})$ and $\Delta S^0{}_{\mathrm{asso}}(\mathrm{C}_n\mathrm{H}_{2n+2})$ leads to a mathematical formulation (eqn (33)), which is compatible with eqn (28).

$$\Delta H^0{}_{\mathrm{asso}}(\mathrm{C}_n\mathrm{H}_{2n+2}) = 295(19)\Delta S^0_{\mathrm{asso}}(\mathrm{C}_n\mathrm{H}_{2n+2}) + 7327(1400)\ \mathrm{J\ mol^{-1}} \quad (33)$$

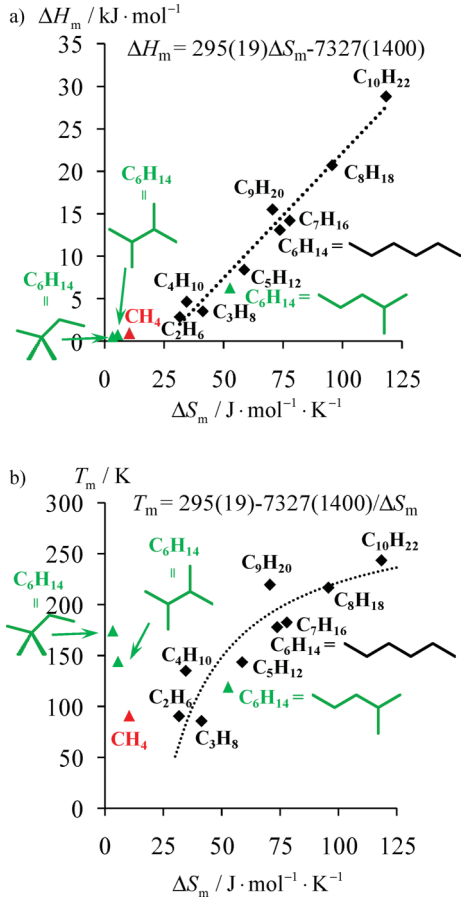

Fig. 5 (a) $\Delta H^0_m(C_nH_{2n+2})$ *vs.* $\Delta S^0_m(C_nH_{2n+2})$ and (b) T_m *vs.* $\Delta S^0_m(C_nH_{2n+2})$ correlation plots for the melting of saturated linear hydrocarbons C_nH_{2n+2} (black: $n \geq 2$; red: $n = 1 = CH_4$; green: branched isomers of *n*-hexane).[28]

The slope of the linear $\Delta H^0_m(C_nH_{2n+2})$ *vs.* $\Delta S^0_m(C_nH_{2n+2})$ plot has Kelvin units and corresponds to the so-called *compensation temperature* ($a = T^{comp}_{asso}(C_nH_{2n+2}) = 295(19)$ K), *i.e.* the temperature at which all association processes are iso-ergonic and display the same *compensation free energy* change $b = \Delta G^{comp}_{asso}(C_nH_{2n+2}) = 7327(1400)$ J mol^{-1}.[29] Consequently, when eqn (28) is experimentally satisfied, it can be rewritten as

$$\Delta H_{asso} = T^{comp}_{asso}\Delta S_{asso} + \Delta G^{comp}_{asso} \quad (34)$$

For the sake of clarity with the mathematical notations, we use here the following approximations $\Delta H_m \simeq \Delta H^0_m$ and $\Delta S_m \simeq \Delta S^0_m$. In other words, we assume that the enthalpy and entropy changes do not significantly depend on the temperature between 298 K (standard conditions) and the incriminated transition temperatures T_m. At the melting temperature, the phase equilibrium condition requires $\Delta G_m = 0$ and we deduce that[27]

$$\Delta G_m = \Delta H^0_m - T_m\Delta S^0_m = 0 \Rightarrow T_m = \frac{\Delta H^0_m}{\Delta S^0_m} = \frac{\Delta H^0_{asso}}{\Delta S^0_{asso}} \quad (35)$$

The introduction of strict H/S compensation (eqn (34)) into eqn (35) yields

$$T_m = T^{comp}_{asso} - \frac{\Delta G^{comp}_{asso}}{\Delta S^0_m} = T^{comp}_{asso} + \frac{\Delta G^{comp}_{asso}}{\Delta S^0_{asso}} \quad (36)$$

or

$$T_m = T^{comp}_{asso}\left(1 + \frac{\Delta G^{comp}_{asso}}{\Delta H^0_m}\right)^{-1} = T^{comp}_{asso}\left(1 - \frac{\Delta G^{comp}_{asso}}{\Delta H^0_{asso}}\right)^{-1} \quad (37)$$

A rapid inspection of eqn (36) and (37) shows that the sign of the compensation free energy change, ΔG^{comp}_{asso}, is crucial for the evolution of the melting temperature with the entropic (eqn (36)) or with the enthalpic (eqn (37)) contributions. Three different situations can be envisioned. (1) When $\Delta G^{comp}_{asso} \gg 0$, a weak cohesion regime operates and T_m increases with ΔS^0_m (eqn (36)) or with ΔH^0_m (eqn (37)), a situation encountered for the melting of linear saturated hydrocarbons containing increasing amounts of methylene rotors (Fig. 5b). (2) When $\Delta G^{comp}_{asso} \approx 0$, the operation of an intermediate cohesion regime de-correlates T_m from ΔS^0_m and ΔG^0_m, and the melting temperature remains invariant upon the imposed perturbation. This trend is observed in silver alkanethiolates complexes $Ag(SC_nH_{2n+1})$ possessing chains of increasing lengths (Fig. 6).[30]

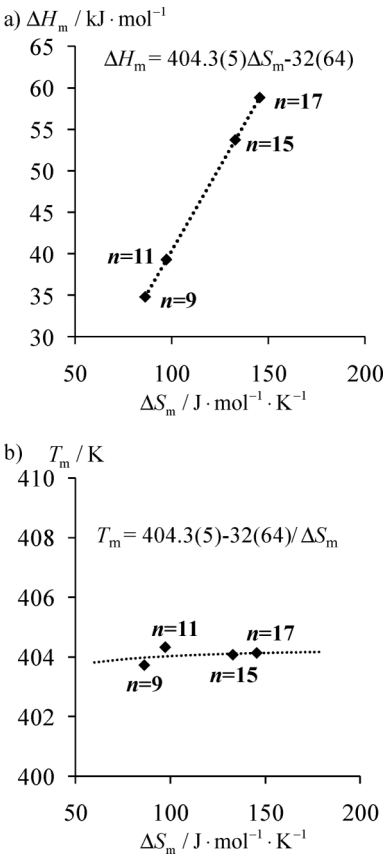

Fig. 6 (a) ΔH^0_m *vs.* ΔS^0_m and (b) T_m *vs.* ΔS^0_m correlation plots for the melting of silver alkanethiolate complexes $Ag(SC_nH_{2n+1})$ ($9 \leq n \leq 17$).[30]

(3) Finally, $\Delta G^{comp}_{asso} \ll 0$ corresponds to a strong cohesion regime, for which a decrease of the melting temperature follows any increase of ΔS^0_m or ΔH^0_m, as illustrated by the melting of polycatenar europium complexes $[Eu(\mathbf{L1^{a-c}})(NO_3)_3]$ grafted with two, six and twelve divergent alkyl chains (Fig. 7).[31] It is worth noting here that the stepwise addition of an increasing number of CH_2 rotors, or of divergent linear alkyl chains induces changes in ΔS^0_m and ΔH^0_m which are roughly proportional with the molecular polarizability, and hence with the molecular weight of the various

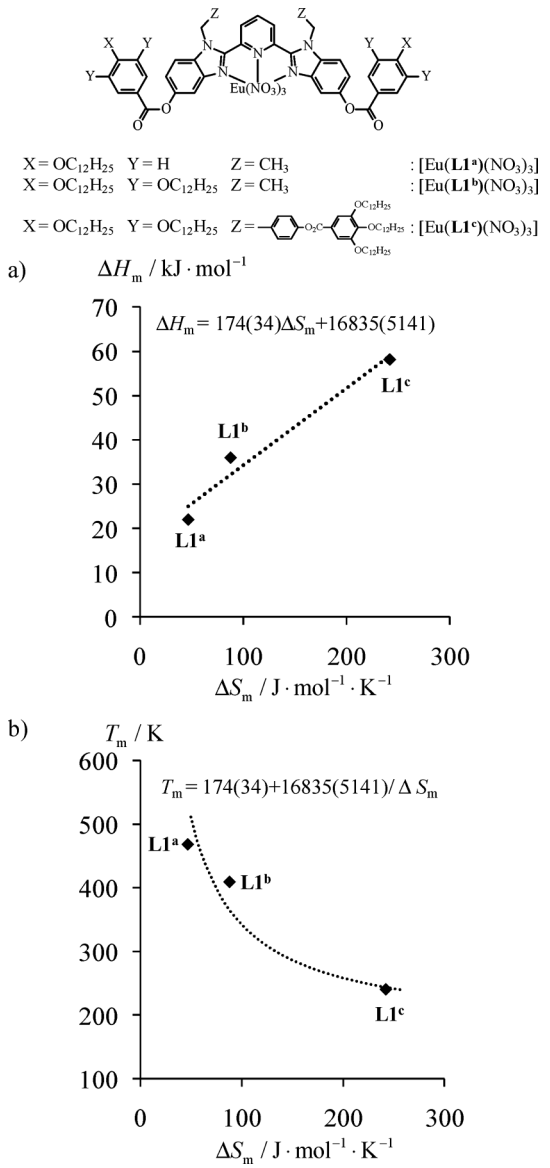

Fig. 7 (a) ΔH^0_m *vs.* ΔS^0_m and (b) T_m *vs.* ΔS^0_m correlation plots for the melting of the polycatenar complexes [Eu(**L1**$^{a-c}$)$(NO_3)_3$].[31]

molecules. Depending on the cohesion regime defined by the sign of ΔG^{comp}_{asso}, we can therefore predict three different behaviours for T_m with increasing molecular weights (T_m increase, stagnate or decrease).

In agreement with the consequences of Ford's model derived in eqn (28)–(30), the linear H/S compensations reported in Fig. 5–7 suggest that the perturbations of the intermolecular interactions brought by the sequential incorporation of additional CH_2 rotors can be caught, for each chemical system, by a single Lennard-Jones potential with a specific contact distance r_0. However, more drastic structural perturbations are expected to induce larger changes in contact distances and/or in force constants with the emergence of significant deviations from linear H/S compensations. Skeleton branching in hexane (Fig. 5, green spots), or symmetrisation in methane (Fig. 5, red spot) are examples which indeed display significant deviations from linearity.

According to a synthetic point of view, H/S compensation can be exploited for the rational tuning of melting temperatures, and liquid crystal engineering is particularly eager for such developments. However, the minor evolution of the melting temperatures (*i.e.* $\Delta G^{comp}_{asso} \approx 0$) with the increasing length of grafted peripheral alkyl chains beyond a critical size, as found in (i) $Ag(SC_nH_{2n+1})$ (Fig. 6, critical length $n \geq 9$), (ii) in the polycatenar series **L2**^{Cn} (critical length $n \geq 8$), **L3**^{Cn} (critical length $n \geq 6$) or **L4**^{Cn} (critical length $n \geq 8$, Fig. 8 and 9)[32] and (iii) in planar neutral Pt(II) hexacatenar complexes,[33] suggests that the classical construction of phase diagrams with alkyl chains of stepwise increasing lengths has only a limited potential for designing room-temperature mesophases. We however notice that the slope of the rough linear H/S correlations estimated for the hexacatenar ligands **L4**^{Cn} is significantly smaller that those found for **L2**^{Cn} and **L3**^{Cn} (Fig. 8a), a trend suggesting different intermolecular interactions (as measured by the $(r_0)^2\kappa_0$ parameter in eqn (29)) in polycatenar systems possessing a large number of diverging alkyl chains. This empirical *polycatenar effect*, systematically exploited for its beneficial consequences on the lowering of melting temperatures,[25,34] indeed finds its thermodynamic origin in the significant changes of these structural characteristics. Since $(r_0)^2\kappa_0$ varies along the series **L2**^{Cn} → **L3**^{Cn} → **L4**^{Cn} for a fixed value of $n = 8$, or of $n = 12$, we predict (and indeed observe) significant deviation from linear H/S correlations for ΔH^0_m *vs.* ΔS^0_m plots measuring the polycatenar effect (Fig. 10a). It is worth stressing here that the polycatenar perturbations analyzed in Fig. 7 and 10, are both characterized by a strong cohesion regime ($\Delta G^{comp}_{asso} \ll 0$), and thus the melting temperatures decrease with increasing molecular weights.

5. Enthalpy–entropy compensation in intermolecular complexation processes occurring in solution

According to Choppin's model for standard intermolecular connections operating in solution (Fig. 1),[11] a desolvation step should precede the target association step. The *n*-merization process of eqn (31) must be adapted for solvation effects, and eqn (38) holds for a simple dimerization occurring in solution ($n = 2$, S is a solvent molecule).

$$2A(S)_m \rightleftharpoons [A_2](S)_p + (2m - p)S;\ \Delta G^{A,S}_{dim} = \Delta H^{A,S}_{dim} - T\Delta S^{A,S}_{dim} \quad (38)$$

The separation of the global intermolecular dimerization into two successive steps yields

$$2A(S)_m \rightleftharpoons 2A(S)_{p/2} + (2m - p)S;\ \Delta G^{A,S}_{desolv} = \Delta H^{A,S}_{desolv} - T\Delta S^{A,S}_{desolv} \quad (39)$$

$$2A(S)_{p/2} \rightleftharpoons [A_2](S)_p;\ \Delta G^{A,S}_{asso} = \Delta H^{A,S}_{asso} - T\Delta S^{A,S}_{asso} \quad (40)$$

Consequently, we can write

$$\Delta G^{A,S}_{dim} = \Delta G^{A,S}_{desolv} + \Delta G^{A,S}_{asso} \quad (41)$$

$$\Delta H^{A,S}_{dim} = \Delta H^{A,S}_{desolv} + \Delta H^{A,S}_{asso} \quad (42)$$

$$\Delta S^{A,S}_{dim} = \Delta S^{A,S}_{desolv} + \Delta S^{A,S}_{asso} \quad (43)$$

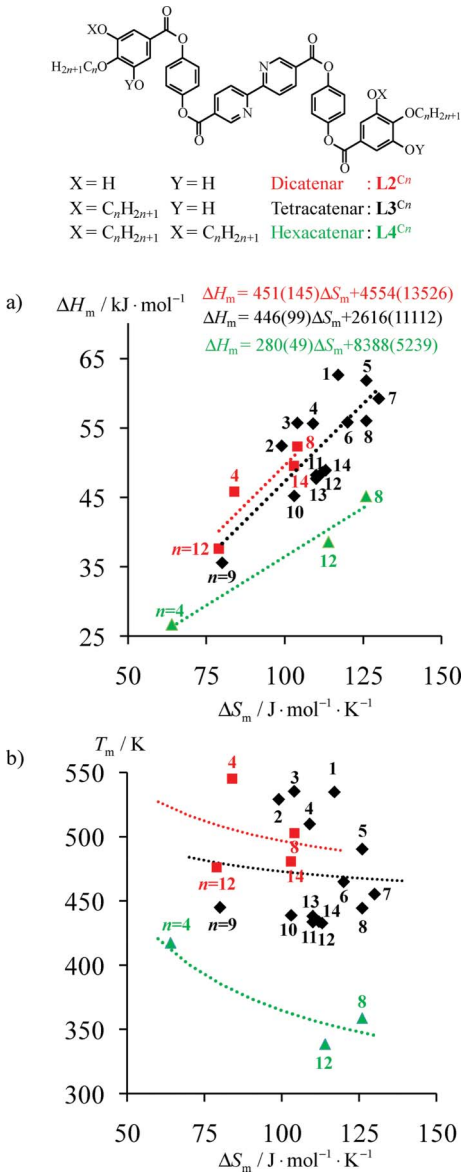

Fig. 8 (a) ΔH^0_m *vs.* ΔS^0_m and (b) T_m *vs.* ΔS^0_m correlation plots for the melting of the polycatenar ligands **L2**^{Cn} (red), **L3**^{Cn} (black) and **L4**^{Cn} (green).[32]

Let's now assume that a minor perturbation is applied to A, so that each intermolecular step (*i.e.* dissociation in eqn (39) and association in eqn (40)) can be modelled with a specific Lennard-Jones potential relying on constant values for r^0_{desolv} and r^0_{asso} within the frame of Ford's model (eqn (28)–(30)). Strict H/S compensation depicted in eqn (34) operates twice and we can write

$$\Delta H^{A,S}_{desolv} = T^{comp}_{desolv}\Delta S^{A,S}_{desolv} + \Delta G^{comp}_{desolv} \quad (44)$$

$$\Delta H^{A,S}_{asso} = T^{comp}_{asso}\Delta S^{A,S}_{asso} + \Delta G^{comp}_{asso} \quad (45)$$

The introduction of eqn (44), (45) into eqn (42) yields

$$\Delta H^{A,S}_{dim} = T^{comp}_{asso}\Delta S^{A,S}_{dim} + \Delta S^{A,S}_{desolv}(T^{comp}_{desolv} - T^{comp}_{asso}) + (\Delta G^{comp}_{desolv} + \Delta G^{comp}_{asso}) \quad (46)$$

A close scrutiny at eqn (46) indicates that, beyond the original structural requirements r^0_{desolv} = constant and r^0_{asso} = constant which must be obeyed along the perturbation, the operation of a linear H/S correlation for intermolecular dimerization in solution only results when at least one of the additional criteria collected in eqn (47)–(49) is fulfilled.

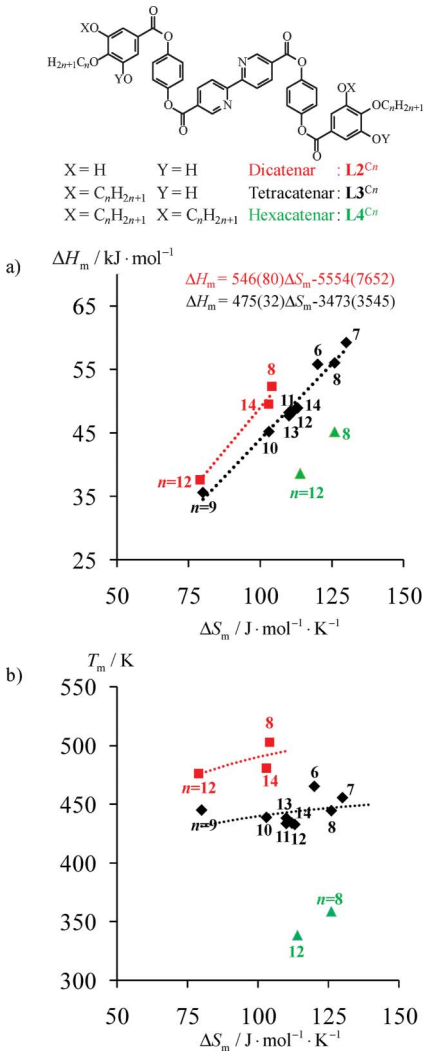

Fig. 9 (a) ΔH^0_m *vs.* ΔS^0_m and (b) T_m *vs.* ΔS^0_m correlation plots beyond critical lengths for the melting of the polycatenar ligands **L2**^{Cn} ($n \geq 8$, red), **L3**^{Cn} ($n \geq 6$, black) and **L4**^{Cn} ($n \geq 8$, green).[32]

$$\Delta S^{A,S}_{desolv} = \text{constant} \quad (47)$$

$$T^{comp}_{desolv} = T^{comp}_{asso} \quad (48)$$

$$\Delta S^{A,S}_{asso} = \gamma\Delta S^{A,S}_{desolv} + \delta \quad (49)$$

The first condition, *i.e.* $\Delta S^{A,S}_{desolv}$ = constant (eqn (47)) has deep chemical roots,[35] and it is matched when the perturbation applied to the complexation process does not significantly affect the entropy changes accompanying the desolvation process. The second condition $T^{comp}_{desolv} = T^{comp}_{asso}$ (eqn (48)) is purely mathematical and it cannot be *a priori* correlated with obvious molecular parameters. However, eqn (48) automatically applies when an empirical linear correlation is detected between $\Delta H^{A,S}_{dim}$ and $\Delta S^{A,S}_{dim}$

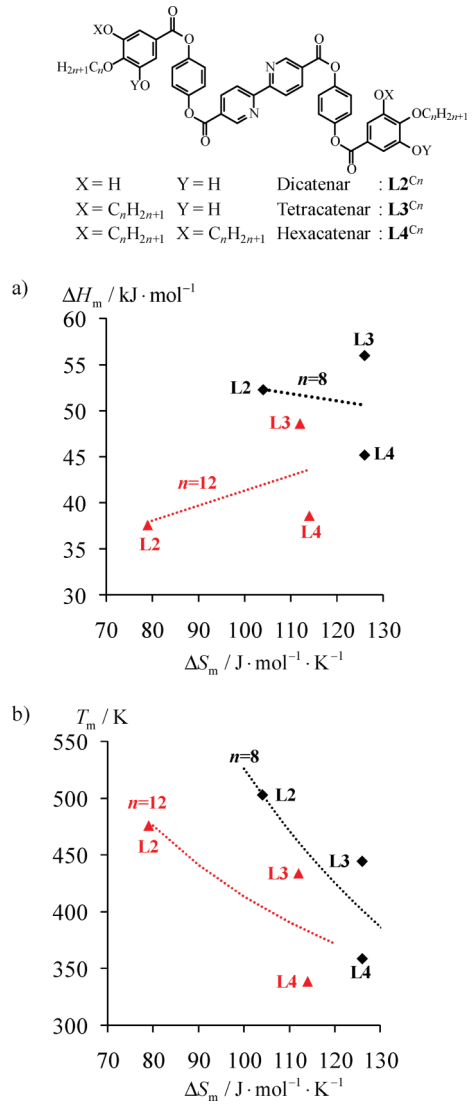

Fig. 10 (a) ΔH^0_m *vs.* ΔS^0_m and (b) T_m *vs.* ΔS^0_m correlation plots for the melting of the ligands $\mathbf{L}k^{C8}$ (black) and $\mathbf{L}k^{C12}$ (red, k = 2–4) highlighting the polycatenar effect.[32]

(*vide supra*, eqn (52)). The last alternative depicted in eqn (49) is clearly the less constraining condition, but, to the best of our knowledge, we cannot foresee any specific chemical behaviour inducing this linear correlation. The introduction of eqn (49) into eqn (46) yields the linear correlation shown in eqn (50) after some algebraic transformations.

$$\Delta H^{A,S}_{dim} = \Delta S^{A,S}_{dim}\left(\frac{\gamma T^{comp}_{asso} + T^{comp}_{desolv}}{\gamma + 1}\right) + \delta\left(\frac{T^{comp}_{asso} - T^{comp}_{desolv}}{\gamma + 1}\right) + \left(\Delta G^{comp}_{desolv} + \Delta G^{comp}_{asso}\right) \quad (50)$$

Depending on the sign and magnitude of γ, both H/S compensation ($(\gamma T^{comp}_{asso} + T^{comp}_{desolv})/(\gamma + 1) > 0$) and anti-compensation ($(\gamma T^{comp}_{asso} + T^{comp}_{desolv})/(\gamma + 1) < 0$) can be predicted when eqn (49) is obeyed.

An intentional test for eqn (46) was recently designed with the thorough thermodynamic investigation of the dimerization of a series of large semi-dendrimeric complexes $[Ln(\mathbf{L6}^{a-j})(NO_3)_3]$ in dichloromethane (eqn (51), Ln = Pr, Eu; Fig. 11 and 12).[21]

$$2\,[Ln(\mathbf{L6}^{a-j})(NO_3)_3] \rightleftharpoons [Ln_2(\mathbf{L6}^{a-j})_2(NO_3)_6];\ \Delta G^{Ln,L6\alpha}_{dim} \quad (51)$$

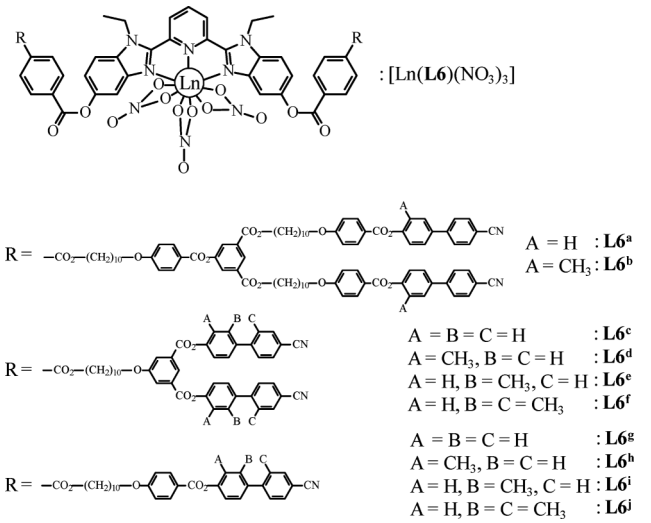

Fig. 11 Chemical structures of the semi-dendrimeric complexes $[Ln(\mathbf{L6}^{a-j})(NO_3)_3]$.[14c]

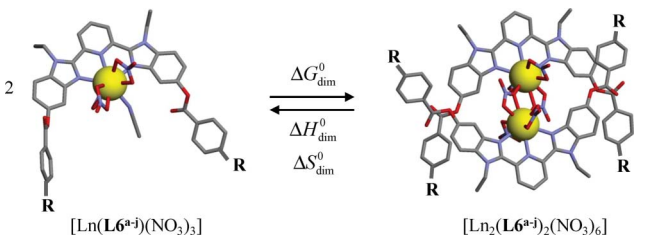

Fig. 12 Schematic dimerization of $[Ln(\mathbf{L6}^{a-j})(NO_3)_3]$ occurring in dichloromethane (eqn (51)). The molecular structures correspond to crystal structures obtained by X-ray diffraction techniques.[21]

The classical Onsager's approach,[35] further substantiated by modern quantum computing techniques,[36] predicts that the solvation free energy change produced by a neutral globular dipolar molecule in a dielectric depends on its molecular volume according to $\Delta G_{solv} \propto (V_{mol})^{-1}$. So, the larger the molecules, the smaller variations of $\Delta\Delta G_{solv}$ along the series, and eqn (47) is obeyed.[14d,37]

After application of the standard criteria for removing artificial correlations resulting from inadequate dissections of the free energy changes $\Delta G^{Ln,L6\alpha}_{dim}$ into enthalpic and entropic contributions by using van't Hoff plots,[38] the residual non-artificial thermodynamic data collected for the dimerization of $[Ln(\mathbf{L6}^{a-j})(NO_3)_3]$ (eqn (51)) indeed display exact H/S compensations along the complete series of ligand in agreement with eqn (46), but with different slopes for each specific metal (Ln = Pr, Eu; Fig. 13).[21] Since the slopes of the ΔH^0_{dim} *vs.* ΔS^0_{dim} correlation plots correspond to the compensation temperature T^{comp}_{asso} (eqn (46)), a parameter which can be theoretically rationalized by using Ford's model as $T^{comp}_{asso} = (1 - 2^{1/6})^2 (r_0)^2 \kappa_0 / 3k_b$ (eqn (29)), we deduce that the observed trend $T^{comp}_{asso,Ln=Pr} = 329(17)$ K > $T^{comp}_{asso,Ln=Pr} = 278(7)$ K can be assigned to a decrease of the minimum intermolecular contact distance r_0

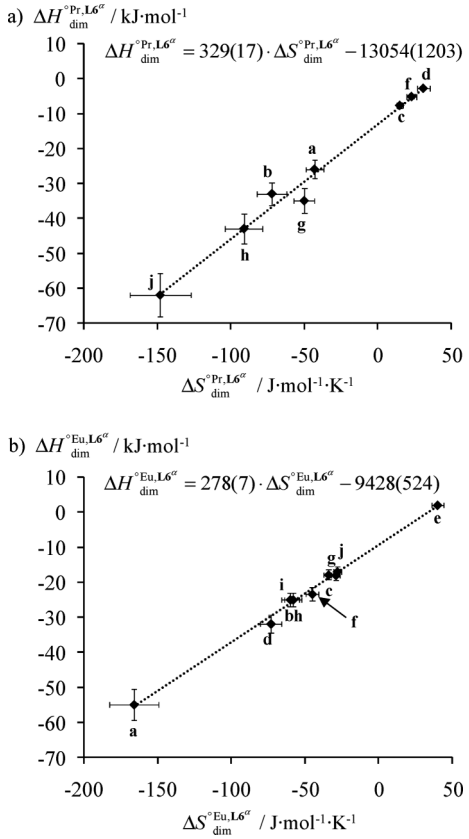

Fig. 13 ΔH^{0}_{dim} *vs.* ΔS^{0}_{dim} correlation plots for the dimerization of (a) $[Pr(\mathbf{L6^{a-j}})(NO_3)_3]$ and (b) $[Eu(\mathbf{L6^{a-j}})(NO_3)_3]$ in dichloromethane (eqn (52)).[21]

for the smaller europium(III) cation, combined with a decrease of the force constant κ_0 resulting from the reluctance of Eu^{3+} to extend its coordination number (*CN*) beyond *CN* = 9 in the dimer $[Ln_2(\mathbf{L6^{a-j}})_2(NO_3)_6]$, which requires *CN* = 10 (Fig. 12).[21]

It is worth noting here that, as soon as a linear *H*/*S* compensation effect is empirically observed for any intermolecular complexation process occurring in solution, the simultaneous consideration of eqn (46) and of its twin form in which $\Delta S^{A,S}_{desolv}$ is replaced with $\Delta S^{A,S}_{desolv} = \Delta S^{A,S}_{dim} - \Delta S^{A,S}_{asso}$ (eqn (52)), implies that $T^{comp}_{desolv} = T^{comp}_{asso}$ (eqn (48)), a simple inference which justifies the interpretation of T^{comp}_{asso} as the crucial structural factor for the dimerization of $[Ln(\mathbf{L6^{a-j}})(NO_3)_3]$ in dichloromethane.

$$\Delta H^{A,S}_{dim} = T^{comp}_{desolv}\Delta S^{A,S}_{dim} + \Delta S^{A,S}_{asso}(T^{comp}_{asso} - T^{comp}_{desolv}) + (\Delta G^{comp}_{desolv} + \Delta G^{comp}_{asso}) \quad (52)$$

Raymond, Bergman and co-workers recently reported on a remarkable *H*/*S* compensation process characterizing the encapsulation of various cationic iridium guests (the choice of the R groups attached to the iridium atom represents the perturbation applied to the system) by an anionic $[Ga_4(\mathbf{L5})_6]^{12-}$ host in various solvents (Fig. 14).[14c] After checking for non-artificial dissection of the free energy changes $\Delta G_{complex}$ into enthalpic $\Delta H^{0}_{complex}$ and entropic $\Delta S^{0}_{complex}$ contributions,[38] the Berkeley's groups established that exact linear $\Delta H^{0}_{complex}$ *vs.* $\Delta S^{0}_{complex}$ compensations occur in water and in methanol. Without referring to eqn (46), these authors used related, but qualitative arguments for analyzing their data, and concluded that the desolvation of the iridium guests in polar aprotic solvents is crucial for observing *H*/*S* compensation, in full agreement with a system obeying eqn (46).

The latter observations, which are in line with a wealth of empirical thermodynamic observations previously collected for association processes occurring in biologic media, indicate that eqn (46) obviously extends beyond strict dimerization processes, and thus holds for any hetero-component intermolecular [AB] interactions according that $\Delta S^{A,S}_{desolv}$ and $\Delta H^{A,S}_{desolv}$ (eqn (39)) are replaced with $\Delta S^{A,B,S}_{desolv}$ and $\Delta H^{A,B,S}_{desolv}$ (eqn (13)), as illustrated in Fig. 1.

Conclusion and outlook

Despite the statistical scepticism[24,38] created by the report for decades of countless *H*/*S* compensation effects for simple intermolecular associations operating in solution, some recent unambiguous separations of enthalpic and entropic contributions firmly established that *H*/*S* correlation was indeed a common issue of intermolecular interactions upon the application of minor electronic and/or structural perturbations.[12,14,17,18,21] However, one can be struck by that, contrary to the express ethical recommendations of the well-respected 17th century scientists Descartes (Discours de la Méthode, 1637) and Newton (Philosophae Naturalis Principa Mathematica, 1686), who claimed that scientific models in experimental sciences should find their essence in some intellectual construction for which all accessible consequences should be derived and checked, experimental *H*/*S* correlations are usually deciphered with the help of purely inductive considerations. In 2005, Ford pointed out this weakness for a large part of *H*/*S* correlations regularly reported in biology and chemistry, and put the bases for an alternative deductive approach using some accessible physical concepts modelling intermolecular interactions.[18] Modelling any standard intermolecular interaction with a simple harmonic potential developed at the minimum of a standard Lennard-Jones (12,6) curve, Ford demonstrated that positive enthalpy–entropy correlations (*i.e. H*/*S* compensations) occur as soon as the minimum intermolecular contact distance r_0 is invariant upon minor perturbations applied to the [AB] pairs (eqn (19), (20) and (24)). When this 'hidden' structural condition

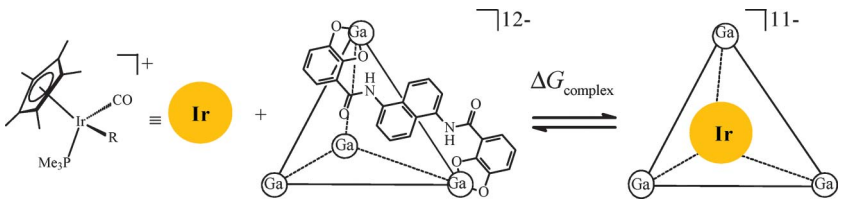

Fig. 14 Encapsulation of iridium guests by $Na_{12}[Ga_4(\mathbf{L5})_6]$ in solution.[14c]

is combined with a limited variation of the magnitude of the force constant $\kappa_0^{A,B}$ characterizing the intermolecular cohesion, strict linear H/S compensations are expected (eqn (28)–(30)). Apparently, this non-sophisticated approach catches the main aspects of a wealth of experimental systems, as exemplified by the evolution of the melting temperatures of saturated hydrocarbons discussed in section 4. It is worth stressing here that, for a single-step association or dissociation process, as that found in the melting of pure solids, linear H/S compensation brings three different trends for the melting temperatures with respect to increasing melting entropies (eqn (36)) or enthalpies (eqn (37)). Since $T_m = T_{asso}^{comp} - \Delta G_{asso}^{comp}/\Delta S_m^0$ (eqn (36)), the sign of the compensation free energy change is crucial and it results in an increase ($\Delta G_{asso}^{comp} > 0$, weak cohesion regime), a stagnation ($\Delta G_{asso}^{comp} \approx 0$, intermediate cohesion regime) or a decrease ($\Delta G_{asso}^{comp} < 0$, strong cohesion regime) of the melting temperatures for increasing melting entropies. As soon as some chemically-intuitive control of ΔG_{asso}^{comp} is at hand for a given perturbation, these predictions can be exploited for the rational tuning of thermal properties in selected materials. For instance, an increase in the number of methylenic rotors within linear saturated hydrocarbons brings a weak cohesion regime and larger melting temperatures are found for the heaviest members of the series (Fig. 5). Alternatively, an intermediate cohesion regime results from the connection of linear alkyl chains of increasing length to a rigid and polarizable aromatic and/or metallic calamitic cores, and the melting temperatures only slightly vary (Fig. 6 and 8). Finally, the dispersion of several alkyl chains at the periphery of aromatic spacers (*i.e.* the polycatenar effect) corresponds to a strong cohesion regime displaying lower melting temperatures for the heavier members of the series (Fig. 7 and 10). Since linear H/S correlations are a simple deduction of some physico-chemical concepts in Ford's model, their slopes T_{asso}^{comp} (eqn (29)) and intercepts ΔG_{asso}^{comp} (eqn (30)) are related to specific and accessible parameters, thus paving the way for some rough (because of the non-sophisticated description of intermolecular interactions in this model), but rational thermodynamic design of intermolecular interactions operating in materials. Despite the above-mentioned appealing consequences brought by H/S compensation for optimizing melting temperatures of solid materials or of liquid crystalline phases, we should keep in mind that these predictions are strictly limited to systems for which the minimum contact distance is fixed (Fig. 15a). As soon as r_0 varies, there is no reason for obtaining any specific H/S correlations and the origin for the reports of several total lack of unambiguous correlations (Fig. 15b) or of anti-compensation (Fig. 15c) can be understood with the consideration of variable compensation temperatures T_{asso}^{comp} and free energies ΔG_{asso}^{comp} characterizing the different members of the series under investigation.[18]

Finally, for a simple intermolecular connection forming a [AB] pair in solution, which represents the elementary building block of innumerable chemical or biological processes, the overall two-step mechanism requires two successive H/S compensation phenomena; the first one controlling the initial desolvation step and the second one mastering the subsequent association step (eqn (44) and (45)). Since these two intermolecular processes are 'structurally' comparable, it is not surprising that, for a given perturbation, the invariance of r_{desolv}^0 (eqn (44)) is combined with that of r_{asso}^0 (eqn (45)), thus favouring the emergence of H/S compensations for connection processes occurring in solution.

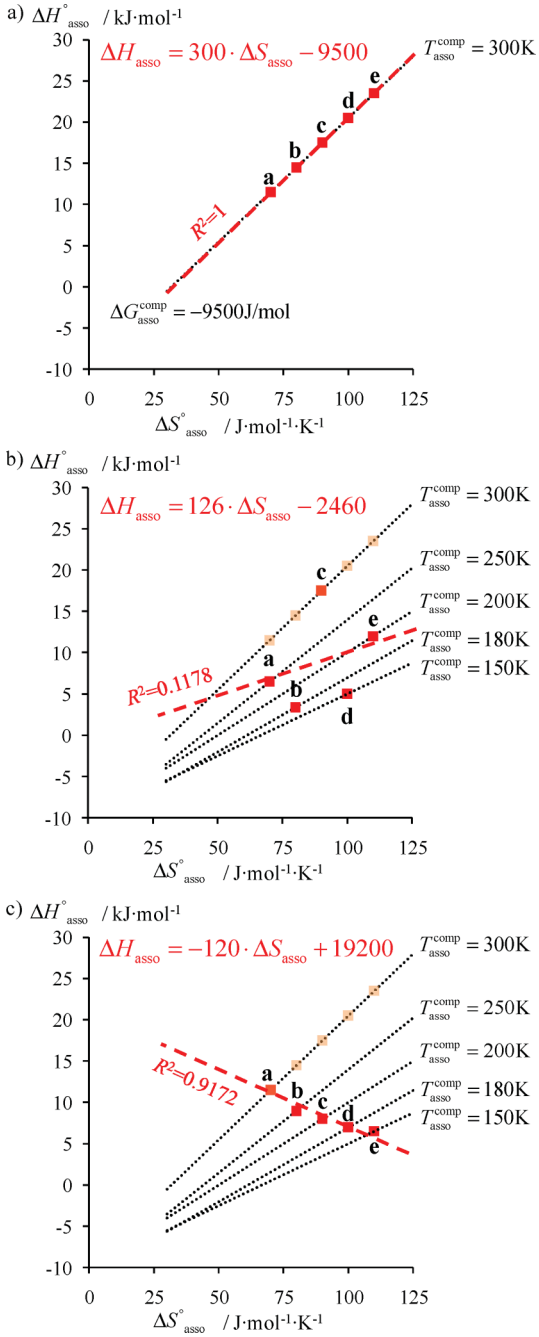

Fig. 15 ΔH_{asso}^0 *vs.* ΔS_{asso}^0 plots illustrating (a) compensation (the minimum contact distance r_0 is invariant for the five members **a**–**e** of the perturbed series with $T_{asso}^{comp} = (1 - 2^{1/6})^2 (r_0)^2 \kappa_0 / 3k_b = 300$ K; eqn (29)), (b) lack of correlation (r_0 randomly varies along the five members **a**–**e** of the perturbed series) and (c) anti-compensation (r_0 systematically decreases along the five members **a**–**e** of the perturbed series).

Though less obvious, the additional condition requiring that $\Delta S_{desolv}^{A,B,S}$ = constant, stated in eqn (46) and (47), is also common for systems undergoing minor perturbations compatible with the above-mentioned invariance of the minimum contact distance. In this context, and within the frame of Ford's model, the slope of linear H/S plots unravelled in solution, provides a direct estimation of the compensation temperature for the pure association step (eqn (46)). This consequence provides a powerful

tool for structurally investigating weak intermolecular cohesion occurring in solution as illustrated in section 5. We are now equipped for considering some extensions of the free-energy thermodynamic self-assembly model discussed in section 1. Let's thus return to the microscopic thermodynamic parameters depicted in eqn (9) and (10) for the replacement of water molecules with ammonia molecules around Ni(II) (eqn (8)). The statistical factors correspond to purely entropic contributions and are not subject to debate.[8] On the contrary, the microscopic hetero-component free energy change $\Delta G_{\text{inter}}^{\text{Ni,NH3}} = -RT \ln(k^{\text{Ni,NH3}})$ characterizing the Ni–NH_3 connection exactly matches the criteria for which one can expect H/S compensations for both desolvation and association steps. For a series of amine NX_3 of increasing size and/or variable electronic density, the dissection of $\Delta G_{\text{inter}}^{\text{Ni,NH3}}$, and of the associated homo-component corrections $\Delta E_{cis}^{\text{NX3,NX3}}$ and $\Delta E_{trans}^{\text{NX3,NX3}}$, into their enthalpic and entropic contributions should contribute to the recognition and manipulation of stereo-electronic criteria controlling (i) the exact role played by the so-called steric bulk for coordination to Ni(II), (ii) the consequences of the effective charges borne by the nitrogen donor atoms onto the Ni–N bond, and (iii) the enthalpic *vs.* entropic origin of cooperativity measured by $\Delta E_{cis}^{\text{NX3,NX3}}$ and $\Delta E_{trans}^{\text{NX3,NX3}}$. Most readers, who have reached this ultimate part of this Perspective, would object that such detailed understanding of the Ni–N interactions is of very limited interest for global science, except for specialists in coordination chemistry, and we fully share their opinion. However, let's apply the same approach to self-assemblies controlling recognition processes in physiology, medicine and biology. A thorough understanding of the underlying intermolecular connection of an effector to a receptor could be at the origin of some novel design for drugs, agonists or antagonist, and of the discovery of the mechanism of their action in term of entropy and enthalpy control.

Acknowledgements

Financial support from the Swiss National Science Foundation is gratefully acknowledged.

References

1 For recent tutorial reviews, see: (*a*) J. Hamacek, M. Borkovec and C. Piguet, *Dalton Trans.*, 2006, 1473; (*b*) P. Thordarson, *Chem. Soc. Rev.*, 2011, **40**, 1305.
2 (*a*) J. Wyman, *Q. Rev. Biophys.*, 1968, **1**, 35; (*b*) J. Hamacek and C. Piguet, *J. Phys. Chem. B*, 2006, **110**, 7783.
3 D. Munro, *Chem. Br.*, 1977, **13**, 100, and references therein.
4 A. V. Hill, *J. Physiol. (London)*, 1910, **4**, 40.
5 G. Scatchard, *Ann. N. Y. Acad. Sci.*, 1949, **51**, 660.
6 (*a*) K. E. Van Holde, *Physical Biochemistry*, Prentice-Hall, Englewood Cliffs, 2nd edn, NJ, 1985; (*b*) B. Perlmutter-Hayman, *Acc. Chem. Res.*, 1986, **19**, 90; (*c*) A. Ben-Naim, *J. Chem. Phys.*, 1998, **108**, 6937; (*d*) C. A. Hunter and H. L. Anderson, *Angew. Chem., Int. Ed.*, 2009, **48**, 7488; (*e*) A. B. C. Deutman, C. Monnereau, M. Moalin, R. G. E. Coumans, N. Veling, M. Coenen, J. M. M. Smits, R. de Gelder, J. A. A. W. Elemans, G. Ercolani, R. J. M. Nolte and A. E. Rowan, *Proc. Natl. Acad. Sci. U. S. A.*, 2009, **106**, 10471.
7 (*a*) G. Koper and M. Borkovec, *J. Phys. Chem. B*, 2001, **105**, 6666; (*b*) M. Borkovec, G. J. M. Koper and C. Piguet, *Curr. Opin. Colloid Interface Sci.*, 2006, **11**, 280.
8 G. Ercolani, C. Piguet, M. Borkovec and J. Hamacek, *J. Phys. Chem. B*, 2007, **111**, 12195.
9 J. Hamacek, M. Borkovec and C. Piguet, *Chem.–Eur. J.*, 2005, **11**, 5217.
10 (*a*) N. Dalla Favera, U. Kiehne, J. Bunzen, S. Hyteballe, A. Lützen and C. Piguet, *Angew. Chem., Int. Ed.*, 2010, **49**, 125; (*b*) C. Piguet, *Chem. Commun.*, 2010, **46**, 6209.
11 G. R. Choppin in *Lanthanide Probes in Life, Chemical and Earth Sciences*, ed. J.-C. G. Bünzli and G. R. Choppin, Elsevier, Amsterdam, 1989, ch. 1, pp. 18–25. Please note that, in Choppin's model, the specific interactions between the liberated solvent molecules with bulk solvent are included within the desolvation step.
12 (*a*) E. Fisicaro, C. Compari and A. Braibanti, *Phys. Chem. Chem. Phys.*, 2004, **6**, 4156; (*b*) D. H. Williams, E. Stephens, D. P. O'Brien and M. Zhou, *Angew. Chem., Int. Ed.*, 2004, **43**, 6596.
13 (*a*) M. S. Searle and D. H. Williams, *J. Am. Chem. Soc.*, 1992, **114**, 10690; (*b*) M. S. Searle, M. S. Westwell and D. H. Williams, *J. Chem. Soc., Perkin Trans. 2*, 1995, 141; (*c*) D. H. Williams, D. P. O'Brien and B. Bardsley, *J. Am. Chem. Soc.*, 2001, **123**, 737.
14 (*a*) F. Bravard, C. Rosset and P. Delangle, *Dalton Trans.*, 2004, 2012; (*b*) P. Di Bernardo, P. L. Zanonato, M. Melchior, R. Portanova, M. Tolazzi, G. Choppin and Z. Wang, *Inorg. Chem.*, 2008, **47**, 1155; (*c*) D. H. Leung, R. G. Bergman and K. N. Raymond, *J. Am. Chem. Soc.*, 2008, **130**, 2798; (*d*) J. Ciupka, X. Cao-Dolg, J. Wiebke and M. Dolg, *Phys. Chem. Chem. Phys.*, 2010, **12**, 13215.
15 (*a*) M. I. Page and W. P. Jencks, *Proc. Natl. Acad. Sci. U. S. A.*, 1971, **68**, 1678; (*b*) W. P. Jencks, *Adv. Enzymol.*, 1975, **43**, 219; (*c*) W. P. Jencks, *Proc. Natl. Acad. Sci. U. S. A.*, 1981, **78**, 4046.
16 D. H. Williams, M. S. Searle, J. P. Mackay, U. Gerhard and R. A. Maplestone, *Proc. Natl. Acad. Sci. U. S. A.*, 1993, **90**, 1172.
17 J. D. Dünitz, *Chem. Biol.*, 1995, **2**, 709.
18 D. M. Ford, *J. Am. Chem. Soc.*, 2005, **127**, 16167.
19 H. B. Luo and K. Sharp, *Proc. Natl. Acad. Sci. U. S. A.*, 2002, **99**, 10399.
20 P. W. Atkins, *Physical Chemistry*, Oxford University Press, Oxford, 5th edn, 1994, pp. A14, 402 and 772.
21 T. B. Jensen, E. Terazzi, K. Buchwalder, L. Guénée, H. Nozary, K. Schenk, B. Heinrich, B. Donnio, D. Guillon and C. Piguet, *Inorg. Chem.*, 2010, **49**, 8601.
22 J. M. Ward, N. M. Gorenstein, J. Tian, S. F. Martin and C. B. Post, *J. Am. Chem. Soc.*, 2010, **132**, 11058.
23 E. B. Starikov and B. Norden, *J. Phys. Chem. B*, 2007, **111**, 14431.
24 A. Cornish-Bowden, *J. Biosci.*, 2002, **27**, 121.
25 A. Escande, L. Guénée, E. Terazzi, T. B. Jensen, H. Nozary and C. Piguet, *Eur. J. Inorg. Chem.*, 2010, 2746, and references therein.
26 (*a*) J. D. Dunitz, *Chem. Commun.*, 2003, 545; (*b*) D. Braga, *Chem. Commun.*, 2003, 2751; (*c*) J. D. Dunitz and A. Gavezzotti, *Chem. Soc. Rev.*, 2009, **38**, 2622.
27 (*a*) B. E. Smith, *Basic Chemical Thermodynamics*, Imperial College Press, London, 5th edn, 2004, p. 42; (*b*) T. Engel and P. Reid, *Physical Chemistry*, Pearson Benjamin Cummings, San Francisco, 2006, ch. 8.
28 D. R. Lide and H. V. Kehiaian, *Handbook of Thermophysical and Thermochemical Data*, CRC Press, Boca Raton, FL, 1994, pp. 99–108.
29 J. E. Leffler, *J. Org. Chem.*, 1955, **20**, 1202.
30 A. A. Levchenko, C. K. Yee, A. N. Parikh and A. Navrotsky, *Chem. Mater.*, 2005, **17**, 5428.
31 (*a*) H. Nozary, C. Piguet, P. Tissot, G. Bernardinelli, J.-C. G. Bünzli, R. Deschenaux and D. Guillon, *J. Am. Chem. Soc.*, 1998, **120**, 12274; (*b*) E. Terazzi, J.-M. Bénech, J.-P. Rivera, G. Bernardinelli, B. Donnio, D. Guillon and C. Piguet, *Dalton Trans.*, 2003, 769; (*c*) E. Terazzi, S. Torelli, G. Bernardinelli, J.-P. Rivera, J.-M. Bénech, C. Bourgogne, B. Donnio, D. Guillon, D. Imbert, J.-C. G. Bünzli, A. Pinto, D. Jeannerat and C. Piguet, *J. Am. Chem. Soc.*, 2005, **127**, 888.
32 K. E. Rowe and D. W. Bruce, *J. Mater. Chem.*, 1998, **8**, 331.
33 C.-T. Liao, H.-H. Chen, H.-F. Hsu, A. Poloek, H.-H. Yeh, Y. Chi, K.-W. Wang, C.-H. Lai, G.-H. Lee, C.-W. Shih and P.-T. Chou, *Chem.–Eur. J.*, 2011, **17**, 546.
34 (*a*) B. Donnio and D. Bruce, *New J. Chem.*, 1999, **23**, 275; (*b*) B. Donnio and D. W. Bruce, *Struct. Bonding*, 1999, **95**, 193; (*c*) R. W. Date, E. Fernandez Iglesias, K. E. Rowe, J. M. Elliott and D. W. Bruce, *Dalton Trans.*, 2003, 1914.

35 (*a*) L. Onsager, *J. Am. Chem. Soc.*, 1936, **58**, 1486; (*b*) D. V. Matyushov, *J. Chem. Phys.*, 2004, **120**, 1375.
36 C. J. Cramer and D. G. Truhlar, *Acc. Chem. Res.*, 2008, **41**, 760, and references therein.
37 (*a*) J. A. Grant, B. T. Pickup, M. J. Sykes, C. A. Kitchen and A. Nicholls, *Phys. Chem. Chem. Phys.*, 2007, **9**, 4913; (*b*) C.-S. Zuo, O. Wiest and Y.-D. Wu, *J. Phys. Chem.*, 2009, **113**, 12028.
38 (*a*) O. Exner, *Nature*, 1964, **201**, 488; (*b*) O. Exner, *Prog. Phys. Org. Chem.*, 1973, **10**, 411; (*c*) R. R. Krug, W. G. Hunter and R. A. Grieger, *Nature*, 1976, **261**, 566; (*d*) R. R. Krug, W. G. Hunter and R. A. Grieger, *J. Phys. Chem.*, 1976, **80**, 2335; (*e*) R. R. Krug, W. G. Hunter and R. A. Grieger, *J. Phys. Chem.*, 1976, **80**, 2341; (*f*) W. Linert and R. F. Jameson, *Chem. Soc. Rev.*, 1989, **18**, 477; (*g*) K. Sharp, *Protein Sci.*, 2001, **10**, 661.